ELSEVIER

Journal of Power Sources 87 (2000) 174–185

JOURNAL OF POWER SOURCES

www.elsevier.com/locate/jpowsour

Random and uncertainty analysis of cylindrical alkaline cells

Y. Zhang, H.Y. Cheh *

Department of Chemical Engineering and Applied Chemistry, Columbia University, New York, NY 10027, USA

Received 2 September 1999; accepted 22 October 1999

Abstract

A method is presented to analyze the performance of a cylindrical $Zn–MnO_2$ alkaline cell with parameter randomness and uncertainties. Two kinds of parameters are recognized with different random and uncertain characteristics. These are parameters with randomness such as the particle size, and parameters with uncertainties such as kinetic and transport coefficients. A sampling procedure based on a differential-algebraic equation model of the alkaline cell is developed to simulate a cell's statistical performance. A numerical example is illustrated with an AA-size cell under a 1 A constant current discharge.

Keywords: Alkaline cells; Statistical analysis; Randomness; Uncertainties

1. Introduction

A systematic study on the modeling of cylindrical alkaline cells has been conducted in our laboratory over the past decade. Mak et al. [1] assumed a quasi-equilibrium process for the cathodic reduction of manganese dioxide in their analysis of the cell behavior under different loads. Satisfactory results were obtained at low rates of discharge. By using the same approach as that of Euler and Nonnenmacher [2], linear kinetics was adopted by Mak et al. [3] to calculate the secondary current distribution in a cylindrical cell geometry. Dimensionless geometric, ohmic and kinetic parameters that controlled the uniformity of current distribution were identified and their effects were calculated quantitatively. A similar analysis based on Butler–Volmer kinetics was performed by Chen and Cheh [4].

When an alkaline cell is being discharged, hydroxide ion is generated in the cathode and consumed in the anode. At high rates of discharge, a high concentration gradient of the hydroxide ion results within the cell and mass transport becomes a critical factor in governing the performance of an alkaline cell. Chen and Cheh [4,5] included mass transport in their model. To include the complex nature of the anode reaction, two anode reaction models were developed; a mixed reaction model which partitioned the anode reaction to either zinc oxidation to form zincate ion or to form solid zinc oxide, and a dissolution–precipitation reaction model which considered the dissolution of zinc to form zincate ion with a subsequent precipitation to form zinc oxide. Both reaction models fitted satisfactorily the experimental discharge results although the dissolution–precipitation reaction model was physically more realistic.

Podlaha and Cheh [6,7] applied Chen and Cheh's model to study cell behavior under both high rates of discharge and under various discharge modes. An important addition of Podlaha and Cheh's analysis [7] was a parameter sensitivity study. By varying one parameter at a time, the effects of four parameters were evaluated.

It is important to note that the majority of the numerical analyses of cell models has been based on the macro-homogeneous theory of porous electrode, utilizing Newman's BAND(J)-type solution technique [8–10]. A more efficient method is the method of lines (MOL) [11]. The typical MOL approach is to discretize the spatial derivatives by finite differences, thereby converting the alkaline cell model to a combination of differential and algebraic equations (DAE) [12]. This approach greatly reduces the magnitude of the problem with much improved accuracy in computation. By calculating the sensitivity coefficients of system variables in terms of the cell parameters and initial conditions with the DAE description,

* Corresponding author. Tel.: +1-212-854-4453; fax: +1-212-854-3054; e-mail: hyc1@columbia.edu

0378-7753/00/$ - see front matter
PII: S0378-7753(99)00471-1

Zhang and Cheh [13] accounted quantitatively the relative importance of these parameters and conditions on the cell performance.

To the best of our knowledge, all cell models in the literature which are based on the macro-homogenous porous electrode theory have assumed deterministic cell conditions. In reality, it happens often that many of the cell parameters possess significant randomness and uncertainties. These randomness and uncertainties arise from manufacturing processes and from inaccuracies in parameter measurements under various conditions [14]. While some parameters lead mainly to variations in real life cell performance, other parameters contribute to variations in the model prediction of cell performance. For instance, the initial cathode porosity may be nonuniform due to the compaction of cathode pellets. The value of the proton diffusivity reported in the literature [15,16] can be different upto several orders of magnitude. Therefore, it is important to have a quantitative evaluation on the effect of parameter randomness and uncertainties on cell model predictions. In this paper, we present a method that predicts the statistical variation of cell performance. A brief summary of our alkaline cell model is given in Appendix A.

2. Cell modeling under parametric randomness and uncertainties

Parameter randomness and uncertainty, in most cases, can be expressed in terms of probabilistic distributions, such as the normal and uniform distribution functions [17]. The probability distribution function defines a range of values and the likelihood of occurrences of each value within the range.

A parameter in the alkaline cell model may have a random value due to uncontrollable manufacturing processes. For example, in all previous alkaline cell models, initial porosities have been considered to be constants in different regions of the cell; the anode, the separator, and the cathode. In reality, these porosities may have variations in both the axial and radial directions in each region. Although it is reasonable to expect that the porosity change during discharge may be random also, we only consider here the initial randomness. With this assumption, a random cell performance can be captured without much loss of accuracy, while avoiding the complexity of adopting a purely stochastic model. Similarly, a parameter may be uncertain when it is estimated or measured experimentally. This uncertainty impacts the confidence level of the model prediction. For both the parameter randomness and uncertainties, a probabilistic distribution function can be used to describe the statistical nature of the parameter. Therefore, the goal of this investigation is to add a stochastic modeling capability for random and uncertainties analysis for the alkaline cell model that has been expressed in a DAE structure [12]. In order to illustrate our revision of the deterministic model, probability distributions were adopted for physical and geometrical parameters, initial conditions, and an operational parameter (Appendix B). Statistical calculations were then performed on system variables (Appendix C).

The DAE form of the alkaline cell model [6] (Appendix A) can be written as follows [12],

$$\begin{cases} \dot{z}_1 = f(z_1, z_2, p, \theta(z_1, z_2)),\ z_1(t_0) = z_{1,0} \\ 0 = \mathbf{A}\, z_2 - g(z_1, z_2, p, \theta(z_1, z_2)) \end{cases} \tag{1}$$

and

$$z_3 = h(z_1, z_2, p, \theta(z_1, z_2)) \tag{2}$$

where:

$z_1 = \left(C_{OH^-}(i)_{i=1,NASC}, C_{Zn(OH)_4^{-2}}(i)_{i=1,NASC}, \varepsilon(i)_{i=1,NASC}, \varepsilon_{Zn}(i)_{i=1,NA}, r_o(i)_{i=1,NC}, X_{MnO_2}(i)_{i=1,NC}\right)$

$z_2 = (i_2(i)_{i=1,NASC}, \eta(i)_{i=1,NASC}, \dot{\upsilon}(i)_{i=1,NASC})$

$z_3 = \left(E_{cell}, C_{H_2O}(i)_{i=1,NASC}, \varepsilon_{ZnO}(i)_{i=1,NA}, r_i(i)_{i=1,NC}, N_{K^+}(i)_{i=1,NASC}, N_{OH^-}(i)_{i=1,NASC}, N_{Zn(OH)_4^{-2}}(i)_{i=1,NASC}, N_{H_2O}(i)_{i=1,NASC}\right)$

$p = \left(\bar{V}_{Zn}, \bar{V}_{ZnO}, \bar{V}_{H_2O}, \bar{V}_{MnOOH}, \bar{V}_{MnO_2}, \text{constants}\right)$

$\theta = \left(D_{KOH}, D_{K_2(OH)_4^{-2}}, K_{KOH}, K_{K_2(OH)_4^{-2}}, k_x, \kappa, \sigma, \varepsilon_{Zn}^0, \varepsilon_{ZnN}^0, \varepsilon_{Hg}, x_{MnO_2}^0, \dot{t}_{OH^-}, \dot{t}_{Zn(OH)_4^{-2}}, \alpha_a, \alpha_c, L_{cell}, r_{ac}, r_a, r_s, r_c, \text{parameters that can be at random or with uncertainty}\right)$

$\mathbf{A}$ = the coefficient matrix after spatial discretization on i_2, η, and $\dot{\upsilon}$

NA = the number of mesh points for the anode

NS = the number of mesh points for the separator

NC = the number of mesh points for the cathode

NASC = NA + NS + NC, the total number of the mesh points in the radial geometry of the cell

The system variables that appeared in Eqs. (1) and (2) are grouped into three categories: z_1 are system variables containing time derivatives, z_2 are system variables determined by algebraic equations only, and z_3 are system variables

calculated after Eqs. (1) and (2) are solved. p represent parameters with constant values, and θ are cell parameters with randomness or uncertainties. For each $\theta_k \in \theta$, it is described by a probability distribution function, $\theta_k = R_U(a_k, b_k)$, or $\theta_k = R_N(\mu_k, \sigma_k)$, where $R_U(a_k, b_k)$ is the uniform distribution over interval (a_k, b_k), and $R_N(\mu_k, \sigma_k)$ is the normal distribution with a mean μ_k and a standard deviation σ_k. Obviously, a parameter may belong to either p or θ, depending on how much is the uncertainty of the parameter and on what impact one may expect from the parameter on the cell performance.

To solve the DAE form of the cell model with parameters defined by distribution functions, a typical procedure is as follows.

1. Specify the uncertainties in select input parameters in terms of probability distributions, such as a normal or uniform distribution.
2. Sample the distribution function defined for each parameter based on whether it is time varying or not. If the parameter is time varying, another sub-sampling procedure at each time step is required until the cell cutoff potential is reached.
3. Calculate the effect of randomness or uncertainties during cell discharge.
4. Apply graphical and statistical techniques to analyze the results.

2.1. Sampling and statistical quantities

The above procedure is a Monte Carlo simulation [18]. While system variables, parameters, and initial conditions are composed of random subsystems that are defined by probability distribution functions, the cell performance is propagated based on the cell model from samplings on each subsystem.

A random value (sample) from a uniform distribution over the interval (a,b) can be obtained from a uniform variate R_U over the interval (0,1) using the following transformation, $Y = (b-a)R_U + a$. In a similar fashion, a random sample for the normal distribution with a mean μ and a standard deviation σ is obtained, $Y = \sigma R_N + \mu$, where R_N is a random value from a normal distribution with parameter $\mu = 0$, and $\sigma = 1$.

Because the cell simulation now involves random values, the results are subject to statistical fluctuations. Thus, the cell performance predicted will not be exact but will have an associated error band. The larger the number of samplings in the simulation, the more precise is the knowledge one acquires about the overall cell performance.

We proceed with choosing N as the sampling number to simulate the statistical cell performance. This means that each parameter with randomness or uncertainty is sampled N times. By propagating a solution of the cell model based on these samplings, each system variable will also present certain statistical characteristics that can be described by, for example, a normal distribution. The evaluation of the confidence interval on the mean of any variable at different times enables one to estimate its precision under a particular sampling size.

Assuming that a variable x (output) obeys a normal distribution, the estimated mean of the variable $\hat{\mu}(t,r)$ along the radial position within the cell can be calculated by taking the average of all solutions at a particular time t based on all N samplings. Accordingly, the standard deviation can be estimated by $s(t,r)$. The precision of the normal distribution parameter, the mean of the variable $\mu(t,r)$, can then be determined by,

$$\mu(t,r) = \bar{x}(t,r) \pm (t_{\mathrm{CL},N-1}) \frac{s(t,r)}{\sqrt{N}} \tag{3}$$

where, $\bar{x}(t,r)$ and $s(t,r)$ are obtained from the simulation based on N samplings, and the $(t_{\mathrm{CL},N-1})$ is the confidence level with values such as 0.90, 0.95, and 0.99. To calculate the relative precision factor over time for a particular variable, the following formula may be adopted,

$$\hat{\mu}_l^{\mathrm{rel}}(r) = (t_{\mathrm{CL},N-1}) \frac{\sum_{j=1}^{N_t} S_l(t_j,r)}{\sqrt{N} \sum_{j=1}^{N_t} |\bar{x}(t_j,r)|} \tag{4}$$

where l is the index for the system variables, and N_t is the total number of time steps. A relative precision factor is the estimated relative error in a statistical prediction. Correspondingly, the overall relative precision factor over time and cell geometry can be computed by,

$$\hat{\mu}_l^{\mathrm{rel}} = \frac{\sum_{k=1}^{N_r} \hat{\mu}_l^{\mathrm{rel}}(r_k)}{N_r} \tag{5}$$

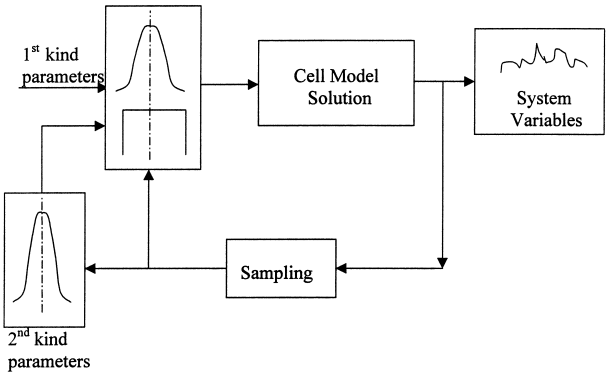

Fig. 1.

where N_r is the total number of mesh points in the radial geometry. Since our cell model involves multiple variables as functions of both the cell geometry and time, we need a universal measure to characterize the average overall precision from the statistical analysis on all the system variables,

$$\hat{\mu}^{\text{rel}}_{\text{model}} = \frac{\sum_{l=1}^{N_l} \hat{\mu}^{\text{rel}}_l}{N_l} \tag{6}$$

where N_l is the total number of system variables.

2.2. Random and uncertainty parameters

In the alkaline cell model, we have identified the two following types of random and uncertain parameters,

1. Random parameters with uncertainties (the first kind), e.g., initial conditions, geometrical parameters and the operational condition such as initial porosities, the radius of anode and the discharge current, etc. (Gaussian distribution),
2. Deterministic parameters with uncertainties (the second kind), e.g., physical parameters such as diffusivities and transference number, etc. (uniform distribution).

Fig. 1 shows a schematic procedure for our calculations. Before a simulation, all parameters were assigned with appropriate distribution functions. For parameters of the first kind, initial sampling was made on its mean. Instead of applying this mean universally for the whole domain of the cell, a further sampling was made to obtain a random profile. Parameters of the second kind were sampled once in each simulation because they bore only uncertainties. In general, several hundred samples on selected variables were needed since there were 15 physical parameters, five geometrical

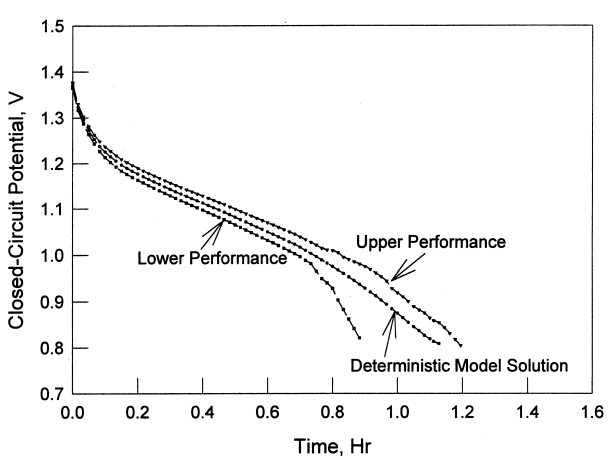

Fig. 2.

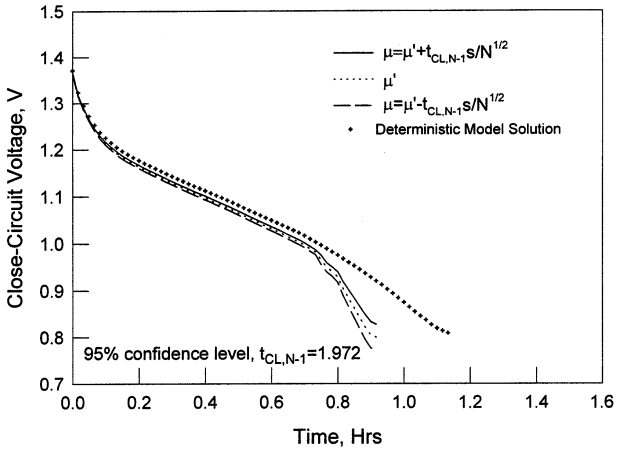

Fig. 3.

parameters, one operational parameter, and six initial conditions that were chosen for our analysis. A list of parameters and initial conditions is given in Appendix B.

3. Results and discussion

To illustrate the application of random and uncertainties analysis, the performance of an AA-size alkaline cell was simulated under parameter randomness and uncertainties at a 1 A constant current discharge.

The 15 physical parameters listed in Appendix B for the simulation were described by uniform distributions. The nominal value for each parameter [6] was taken as the median of the distribution. The uncertainty in the parameter is given either according to the confidence level, or by assumption. In the simulation, all parameters were assumed to have a 10% uncertainty, except for the following parameters: the threshold of precipitation, the diffusivity of $K_2Zn(OH)_4$, and the diffusivity of H^+ within MnO_2 particles with 5%, 50%, and 50% uncertainties, respectively.

The six initial conditions listed in Appendix B were described by normal distributions where the means were determined by their nominal values [6], and the standard deviations were 10^{-4} mol/cm^3 for the initial concentrations, 5×10^{-2} for the initial porosities, and 5×10^{-6} cm for the initial radii of MnO_2 particles.

The five geometrical parameters listed in Appendix B were also considered to have uncertainties. They were assumed to obey normal distributions, for which the means were given by their nominal values [6], and standard deviations were assumed to be 10^{-4} cm for all the cell radii, and 10^{-3} cm for the effective cell length. It was expected that in practical systems, the variations of these parameters were low as compared with other parameters.

Since the discharge current, *I*, could not be held totally constant during discharge, it was assumed to have a normal distribution with a mean of 1 A, and a standard deviation of 0.05 A. In any event, if one should decide that the discharge is

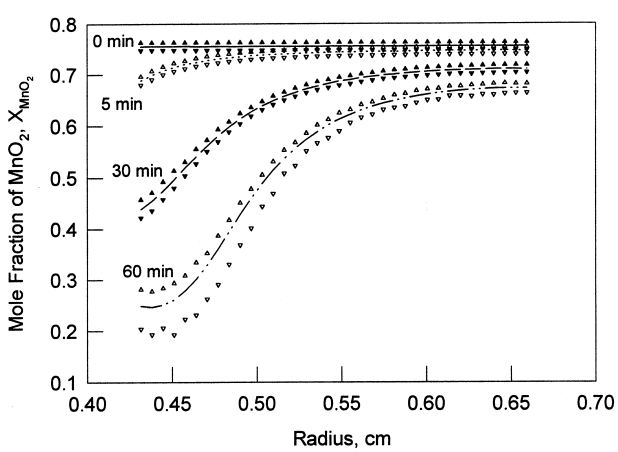

Fig. 4.

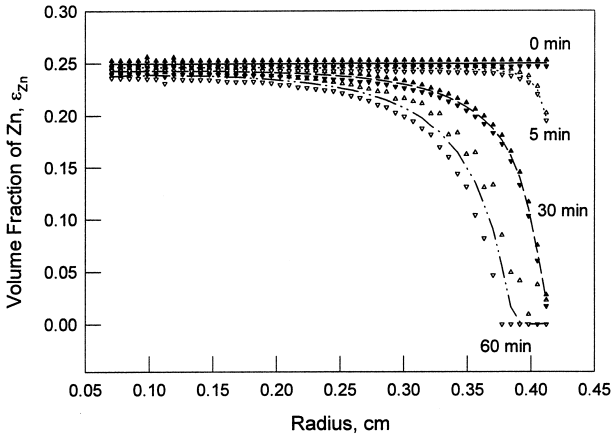

Fig. 5.

under perfect control, it is always possible to remove it from the θ list and put it into the p list. This same approach can be applied to all other parameters.

A statistical simulation based on the above setup of the parameters and the initial conditions was performed on the 17 system variables summarized in Appendix C. Fig. 2 shows a range of the change in the closed-circuit potential (CCP) after 200 samplings. The middle curve represents the solution under the nominal cell conditions solved by the deterministic model. The upper and lower curves represent the maximum and minimum cell performances predicted by the statistical model. Statistically, it was seen that the deterministic model predicted a median of the overall cell performance. Fig. 3 shows statistically the average cell performance (Eq. (3)) and its precision factor $\hat{\mu}^{\text{rel}}_{\text{CCP}}(t)$ (Eq. (4)) with 200 samplings. According to Eq. (5), the overall relative average precision factor $\hat{\mu}^{\text{rel}}_{\text{CCP}}$ is 0.51% with a confidence level at 95%. The results are significant in two ways. First, it provides information on the accuracy of the prediction by the deterministic cell model. Second and possibly more important, it explains the difference in cell performance from manufacturing processes. In fact, the average statistical cell performance under a constant 1 A discharge in Fig. 3 shows the better prediction using the statistical model than that using the deterministic model [6,12]. In this case, the deterministic model overpredicts the cell performance by 10% to 15%.

We have computed the statistical variation of all system variables. For example, Figs. 4 and 5 show the results on the usage of active materials within the cell, the variation of the mole fraction of MnO_2 in the cathode solid mix and the volume fraction of Zn in the anode upon discharge. The relative average precisions (Eq. (5)) for both species have been calculated to be 0.33%, and 2.98%, respectively. The overall relative average precision factor, $\hat{\mu}^{\text{rel}}_{\text{model}}$ (Eq. (6)), for all 17 system variables with 200 samples is found to be 1.39% with a confidence level of 95%.

4. Conclusions

A statistical analysis based on the DAE form of the cell model has been conducted to deal with randomness and uncertainties in system variables and parameters. By defining statistical functions on each of the variables and parameters, a sampling procedure is established.

The analysis based on the statistical method enables us to verify results from the deterministic cell model. It also helps us to identify a realistic range of cell performances. The results of this type of analysis should be useful in identifying controlling parameters to improve the cell uniformity in process design and manufacturing.

Appendix A. Modeling of cylindrical Zn–MnO_2 alkaline cell

A.1. Chemistry of Zn–MnO_2 alkaline cell

The dissociation of KOH and $K_2Zn(OH)_4$ are represented by,

$$\text{(a)}\ \ KOH \rightarrow K + OH^- \tag{A1}$$

$$\text{(b)}\ \ K_2Zn(OH)_4 \rightarrow 2K^+ + (OH)_4^{-2}. \tag{A2}$$

The insoluble species involved in the reactions are Zn and ZnO at the anode, and MnO_2 and MnOOH at the cathode.

Anode:

$$Zn + 4OH^- \rightarrow Zn(OH)_4^{-2} + 2e^- \quad \text{Dissolution} \tag{A3}$$

$$Zn(OH)_4^{-2} \rightarrow ZnO + H_2O + 2OH^- \quad \text{Precipitation} \tag{A4}$$

Cathode:

$$MnO_2 + H_2O + e^- \rightarrow MnOOH + OH^- \quad \text{Single electron transfer} \tag{A5}$$

A.2. Charge balance

The total current of the cell, I, relates to i_1 and i_2 by

$$i_1 + i_2 = \frac{I}{2\pi rL} \tag{A6}$$

A.3. Overpotential

The overpotential η, defined as the local potential difference between the two phases of the porous electrode, is determined by the following equation.

$$\nabla\eta = i_2\left[\frac{1}{\kappa} + \frac{1}{\sigma}\right] - \frac{I}{2\pi rL\sigma} + \frac{\nu_a RT}{F}\left[\frac{s_{OH^-,re,A}}{n_{re}\nu^a_{OH^-}} + \frac{t^{\cdot}_{OH^-}}{z_{OH^-}\nu^a_{OH^-}} - \frac{s_{H_2O,re,A}C_a}{C_{H_2O}}\right]\nabla\ln\left(C_a f_{\pm,a} a^{\theta}_{\pm,a}\right)$$
$$+ \frac{\nu_b RT}{F}\left[\frac{s_{Zn(OH)_4^{-2},re,A}}{n_{re}\nu^b_{Zn(OH)_4^{-2}}} + \frac{t^{\cdot}_{Zn(OH)_4^{-2}}}{z_{Zn(OH)_4^{-2}}\nu^b_{Zn(OH)_4^{-2}}} - \frac{s_{H_2O,re,A}C_b}{C_{H_2O}}\right]\nabla\ln\left(C_b f_{\pm,b} a^{\theta}_{\pm,b}\right) + \frac{RT}{nF}\sum_i s_{i,A}\nabla\ln X_{i,A} \tag{A7}$$

A.4. Kinetics

The rate of electrochemical reaction is represented by the Butler–Volmer equation.

Anode [19]:

$$j = \left(\frac{\partial i_2}{\partial r} + \frac{i_2}{r}\right) = a_a i_{0,ref,a}\left[\begin{array}{l}\left(\dfrac{C_{Zn(OH)_4^{-2},s}}{C_{Zn(OH)_4^{-2},ref}}\right)^{0.06}\left(\dfrac{C_{OH^-,s}}{C_{OH^-,ref}}\right)^{2.59} e^{(1-\alpha_a)2F\eta/RT} \\ -\left(\dfrac{C_{Zn(OH)_4^{-2},s}}{C_{Zn(OH)_4^{-2},ref}}\right)^{0.94}\left(\dfrac{C_{OH^-,s}}{C_{OH^-,ref}}\right)^{-0.92} e^{-\alpha_a 2F\eta/RT}\end{array}\right] \tag{A8}$$

Cathode [4,5,20]:

$$\left(\frac{\partial i_2}{\partial r} + \frac{i_2}{r}\right) = -\frac{e^{(1-\alpha_c)F\eta/RT} - e^{-\alpha_c F\eta/RT}}{\dfrac{1}{a_c i_{0,ref,c}} - \dfrac{e^{-\alpha_c F\eta/RT}}{\dfrac{4\pi FND_{H^+}C_{H^+,b}}{\dfrac{1}{r_o} - \dfrac{1}{r_i}}}} \tag{A9}$$

where $C_{H^+,b} = C_{OH^-}$, $a_c = (4\pi r_i^2)N$, $N = (W/V_c)/\{(4/3)\pi r_o^{0^3}\}d$.

A.5. Electrochemical and chemical reactions

An electrochemical reaction in the cell (subscript A) is the reaction that accepts or releases electrons. Its rate is determined by the Faraday's Law:

$$R_{i,\mathrm{A}} = -\frac{s_{i,\mathrm{A}}}{nF}\nabla\cdot i_2 \tag{A10}$$

A chemical reaction (subscript B) in the cell is the precipitation of ZnO from a supersaturated $Zn(OH)_4^{-2}$ solution.

$$R_{i,\mathrm{B}} = s_{i,\mathrm{B}}\cdot a\cdot k_{\mathrm{s}}\left(C_{\mathrm{Zn(OH)_4^{-2}}} - \xi C^{\mathrm{eq}}_{\mathrm{Zn(OH)_4^{-2}}}\right) \tag{A11}$$

A.6. Fluxes

The flux expression of a species in a concentrated, multicomponent system is derived from a linear sum of frictional interactions exerted on the species by others. Along with the definition of the volumetric average velocity, $v = \sum_i N_i\overline{V}_i$, and by using $i_2 = F\sum_i z_i N_i$, the fluxes of species in a ternary system are described as follows [8].

$$N_{\mathrm{K^+}} = -\left(\nu^{\mathrm{a}}_{\mathrm{K^+}}\varepsilon^{1.5}D_{\mathrm{a,a}} + \nu^{\mathrm{b}}_{\mathrm{K^+}}\varepsilon^{1.5}D_{\mathrm{b,a}}\right)\nabla C_{\mathrm{a}} - \left(\nu^{\mathrm{a}}_{\mathrm{K^+}}\varepsilon^{1.5}D_{\mathrm{a,b}} + \nu^{\mathrm{b}}_{\mathrm{K^+}}\varepsilon^{1.5}D_{\mathrm{b,b}}\right)\nabla C_{\mathrm{b}} + \frac{i_2 t^{\cdot}_{\mathrm{K^+}}}{z_{\mathrm{K^+}}F} + \left(\nu^{\mathrm{a}}_{\mathrm{K^+}}C_{\mathrm{a}} + \nu^{\mathrm{b}}_{\mathrm{K^+}}C_{\mathrm{b}}\right)v^{\cdot} \tag{A12}$$

$$N_{\mathrm{OH^-}} = -\nu^{\mathrm{a}}_{\mathrm{OH^-}}\varepsilon^{1.5}D_{\mathrm{a,a}}\nabla C_{\mathrm{a}} - \nu^{\mathrm{a}}_{\mathrm{OH^-}}\varepsilon^{1.5}D_{\mathrm{a,b}}\nabla C_{\mathrm{b}} + \frac{i_2 t^{\cdot}_{\mathrm{OH^-}}}{z_{\mathrm{OH^-}}F} + \nu^{\mathrm{a}}_{\mathrm{OH^-}}C_{\mathrm{a}}v^{\cdot} \tag{A13}$$

$$N_{\mathrm{Zn(OH)_4^{-2}}} = -\nu^{\mathrm{b}}_{\mathrm{Zn(OH)_4^{-2}}}\varepsilon^{1.5}D_{\mathrm{b,a}}\nabla C_{\mathrm{a}} - \nu^{\mathrm{b}}_{\mathrm{Zn(OH)_4^{-2}}}\varepsilon^{1.5}D_{\mathrm{b,b}}\nabla C_{\mathrm{b}} + \frac{i_2 t^{\cdot}_{\mathrm{Zn(OH)_4^{-2}}}}{z_{\mathrm{Zn(OH)_4^{-2}}}F} + \nu^{\mathrm{b}}_{\mathrm{Zn(OH)_4^{-2}}}C_{\mathrm{b}}v^{\cdot} \tag{A14}$$

$$N_{\mathrm{H_2O}} = -\varepsilon^{1.5}D_{\mathrm{a,a}}\nabla C_{\mathrm{H_2O}} - \varepsilon^{1.5}D_{\mathrm{b,b}}\nabla C_{\mathrm{H_2O}} + C_{\mathrm{H_2O}}v^{\cdot} \tag{A15}$$

A.7. Material balance in porous medium

The material balances of ion species are

$$\frac{\partial\varepsilon C_{\mathrm{OH^-}}}{\partial t} = \nabla\cdot\left(\nu^{\mathrm{a}}_{\mathrm{OH^-}}\varepsilon^{1.5}D_{\mathrm{a,a}}\nabla C_{\mathrm{OH^-}}\right) - \frac{\left(nt^{\cdot}_{\mathrm{OH^-}} + s_{\mathrm{OH^-,A}}z_{\mathrm{OH^-}}\right)}{nz_{\mathrm{OH^-}}F}\nabla\cdot i_2 - \nabla\cdot\left(\nu^{\mathrm{a}}_{\mathrm{OH^-}}C_{\mathrm{OH^-}}v^{\cdot}\right) + s_{\mathrm{OH^-,B}}ak_{\mathrm{s}}\left(C_{\mathrm{Zn(OH)_4^{-2}}} - \xi C^{\mathrm{eq}}_{\mathrm{Zn(OH)_4^{-2}}}\right) \tag{A16}$$

$$\frac{\partial\varepsilon C_{\mathrm{Zn(OH)_4^{-2}}}}{\partial t} = \nabla\cdot\left(\nu^{\mathrm{b}}_{\mathrm{Zn(OH)_4^{-2}}}\varepsilon^{1.5}D_{\mathrm{b,b}}\nabla C_{\mathrm{Zn(OH)_4^{-2}}}\right) - \frac{\left(nt^{\cdot}_{\mathrm{Zn(OH)_4^{-2}}} + s_{\mathrm{Zn(OH)_4^{-2},A}}z_{\mathrm{Zn(OH)_4^{-2}}}\right)}{nz_{\mathrm{Zn(OH)_4^{-2}}}F}\nabla\cdot i_2 - \nabla\cdot\left(\nu^{\mathrm{b}}_{\mathrm{Zn(OH)_4^{-2}}}C_{\mathrm{Zn(OH)_4^{-2}}}v^{\cdot}\right) + s_{\mathrm{Zn(OH)_4^{-2},B}}ak_{\mathrm{s}}\left(C_{\mathrm{Zn(OH)_4^{-2}}} - \xi C^{\mathrm{eq}}_{\mathrm{Zn(OH)_4^{-2}}}\right) \tag{A17}$$

A.8. Stoichiometry

With the reaction stoichiometry and solution neutrality, $C_{\mathrm{H_2O}}$ can be calculated after both $C_{\mathrm{OH^-}}$ and $C_{\mathrm{Zn(OH)_4^{-2}}}$ have been determined.

$$C_{\mathrm{H_2O}} = \frac{1 - \overline{V}_{\mathrm{KOH}}C_{\mathrm{OH^-}}/\nu^{a}_{\mathrm{OH^-}} - \overline{V}_{\mathrm{K_2Zn(OH)_4}}C_{\mathrm{Zn(OH)_4^{-2}}}/\nu^{b}_{\mathrm{Zn(OH)_4^{-2}}}}{\overline{V}_{\mathrm{H_2O}}} \tag{A18}$$

A.9. Porosity

The porosity is calculated from an overall material balance of both the electrochemical reaction and the chemical reaction,

$$\frac{\partial\varepsilon}{\partial t} = -\sum_{\text{solid phase}} R_{i,\mathrm{A}}\overline{V}_{i,\mathrm{A}} - \sum_{\text{solid phase}} R_{i,\mathrm{B}}\overline{V}_{i,\mathrm{B}} = \sum_i \frac{s_{i,\mathrm{A}}\overline{V}_{i,\mathrm{A}}}{nF}\nabla\cdot i_2 - \sum_i s_{i,\mathrm{B}}\overline{V}_{i,\mathrm{B}}ak_{\mathrm{s}}\left(C_{\mathrm{Zn(OH)_4^{-2}}} - \xi C^{\mathrm{eq}}_{\mathrm{Zn(OH)_4^{-2}}}\right) \tag{A19}$$

A.10. Volume average velocity

A combination of the three equations for material balance, stoichiometry, and porosity leads to the following relation for calculating the volume average velocity,

$$(\nabla\cdot\mathbf{v}^{\cdot}) = \underbrace{-\sum_i \frac{s_{i,A}\bar{V}_{i,A}}{nF}\nabla\cdot\mathbf{i} - \sum_i s_{i,B}\bar{V}_{i,B}ak_s\left(C_{Zn(OH)_4^{-2}} - \xi C^{eq}_{Zn(OH)_4^{-2}}\right)}_{\frac{\partial\varepsilon}{\partial t}}$$
$$+ \underbrace{\left[-\frac{\bar{V}_a\left(nt^{\cdot}_{OH^-} + s_{OH^-,A}z_{OH^-}\right)}{v^a_{OH^-}z_{OH^-}} - \frac{\bar{V}_b\left(nt^{\cdot}_{Zn(OH)_4^{-2}} + s_{Zn(OH)_4^{-2},A}z_{Zn(OH)_4^{-2}}\right)}{v^b_{Zn(OH)_4^{-2}}z_{Zn(OH)_4^{-2}}} - \bar{V}_{H_2O}s_{H_2O,A}\right]\cdot\frac{\nabla\cdot\mathbf{i}_2}{nF}}_{\text{Migration term}} \quad \text{(A20)}$$
$$+ \underbrace{\left(\frac{\bar{V}_a}{v^a_{OH^-}}s_{OH^-,B} + \frac{\bar{V}_b}{v^b_{Zn(OH)_4^{-2}}}s_{Zn(OH)_4^{-2},B} + \bar{V}_{H_2O}s_{H_2O,B}\right)ak_s\left(C_{Zn(OH)_4^{-2}} - \xi C^{eq}_{Zn(OH)_4^{-2}}\right)}_{\text{Chemical reaction term}}$$

A.11. Closed-circuit potential of the cell

The closed-circuit potential (CCP), $E_{cell}(t)$, is given by

$$E_{cell}(t) = \underbrace{E_0 + \frac{2RT}{F}\ln\left[\frac{1-f}{f}\right]}_{\substack{E_{ocp}\text{: the open circuit potential} \\ (=1.6\text{ V at }25^{\circ}\text{C})}} + \eta_{cathode} - \eta_{anode} \quad \text{(A21)}$$

Appendix B. Parameters considered with randomness and uncertainties

Physical parameters

$i_{0,ref,a}$	anodic exchange current density (A/cm^2)
$i_{0,ref,c}$	cathodic exchange current density (A/cm^2)
ξ	threshold of precipitation
$D_{K_2Zn(OH)_4}$	diffusivity of potassium zincate (cm^2/s)
D_{H^+}	diffusivity of hydrogen ion (cm^2/s)
K_{KOH}	mass transfer coefficient of potassium hydroxide (cm/s)
$K_{K_2Zn(OH)_4}$	mass transfer coefficient of potassium zincate (cm/s)
k_x	rate constant of precipitation reaction (cm/s)
a_a	specific surface area of anode (cm^{-1})
a_s	specific surface of separator (cm^{-1})
t_{OH^-}	transference number of hydroxide ion
$t_{Zn(OH)_4^{-2}}$	transference number of zincate ion
α_a	anodic transfer coefficient
α_c	cathodic transfer coefficient
σ_c	matrix conductivity of cathode (Ω^{-1} cm^{-1})

Geometrical parameters

L_{eff}	effective discharge length of the cell (cm)
r_{acc}	radius of the anode current collector (cm)
r_a	radius of the anode–separator interface (cm)
r_s	radius of the separator–cathode interface (cm)
r_c	radius of the cathode current collector (cm)

Operational parameter

I	discharge current (A)

Initial conditions

$C^0_{OH^-}$	concentration of hydroxide ion (mol/cm^3)
$C^0_{Zn(OH)_4^{-2}}$	concentration of zincate ion (mol/cm^3)
ε^0_a	porosity of anode
ε^0_s	porosity of separator
ε^0_c	porosity of cathode
r^0_o	radius of manganese dioxide particle (cm)

Appendix C. System variables applied with statistical analysis

C_{OH^-}	concentration of hydroxide ion (mol/cm^3)
$C_{Zn(OH)_4^{-2}}$	concentration of zincate ion (mol/cm^3)
i_2	current density (A/cm^2)
ε	porosity
η	overpotential (V)
υ	volumetric average velocity (cm/s)
ε_{Zn}	volume fraction of zinc
r_o	radius of manganese dioxide particle plus manganese oxyhydroxide layer (cm)
X_{MnO_2}	mole fraction of manganese dioxide
E_{cell}	closed-circuit potential (V)
C_{H_2O}	concentration of water (mol/cm^3)
ε_{ZnO}	volume fraction of zinc oxide
N_{K^+}	flux of potassium ion (mol/cm^2 s)
N_{OH^-}	flux of hydroxide ion (mol/cm^2 s)
$N_{Zn(OH)_4^{-2}}$	flux of zincate ion (mol/cm^2 s)
N_{H_2O}	flux of water (mol/cm^2 s)
r_i	radius of manganese dioxide particles (cm)

C.1. List of symbols

a	specific surface area of anode (cm^{-1})
$a^\theta_\pm$	mean activity coefficient of the electrolyte measured at a secondary reference state
C	specie concentration (mol/cm^3)
$C_{i,s}$	surface concentration of the ith species (mol/cm^3)
$C_{i,ref}$	concentration of the ith species at the reference condition (mol/cm^3)
C_{OH^-}	concentration of OH^- (mol/cm^3)
$C_{Zn(OH)_4^{-2}}$	concentration of $Zn(OH)_4^{-2}$ (mol/cm^3)
$C^{eq}_{Zn(OH)_4^{-2}}$	equilibrium concentration of $Zn(OH)_4^{-2}$ in KOH solution (mol/cm^3)
D	diffusion coefficient (cm^2/s)
$E_{cell}(t)$	closed-circuit potential (CCP) (V)
f	extent of discharge of the cathode, $f=(1/Q)\int_0^t I(t)\mathrm{d}t$
$f_\pm$	mean molar activity coefficient of the electrolyte
E_0	open circuit potential after 50% discharge (V)
E_{ocp}	open circuit potential (= 1.6 V at 25°C) (V)
F	Faraday constant.
$i_{0,ref}$	exchange current density at the reference condition (A/cm^2)
i_1	current density in the matrix phase (A)
i_2	current density (i_2) in the solution phase (A)
I	discharge current of the cell (A)
j	transfer current per unit electrode volume (A/cm^3)
k_s	rate constant of the surface reaction (mol/s)
L	cell length (cm)

n	number of electrons transferred during reaction
N_i	molar fluxes of species i (mol/cm^2 s)
N	equivalent number of spherical particles in cathode, total number of samples
Q	theoretical capacity of MnO_2 in the cathode (A h/g MnO_2)
R	gas constant (8.314 J/K mol)
$R_{i,A}$	volumetric production rate of species i in electrochemical reaction (mol/cm^3 s)
$R_{i,B}$	volumetric production rate of species i in chemical reaction (mol/cm^3 s)
r	radial coordinate from the center of the cell (cm)
s	stoichiometry coefficient of reaction, estimated standard deviation
$s_{i,B}$	stoichiometric coefficient of species i in the chemical reaction
t	time (s)
$t^{\cdot}$	transference number with respect to the volume average velocity
$v^{\cdot}$	volume average velocity (cm/s)
V_c	volume of active material in the cathode (cm^3)
$\bar{V}_i$	partial molar volume of the ith species (cm^3/mol)
W	weight of cathodic active material (g)
$X_{i,A}$	mole fraction of the ith solid species in electrochemical reaction
z	charge number

Greek

α	transfer coefficient
ε	porosity
η	overpotential (V)
η_s	surface overpotential (V)
κ	conductivity of the solution (Ω^{-1} cm^{-1})
μ	mean
ν	stoichiometric coefficient of dissociation
ξ	precipitation threshold ($=3.0$)
σ	conductivity of the matrix (Ω^{-1} cm^{-1}), standard deviation
ϕ_1	potential of the matrix phase (V)
ϕ_2	potential of the electrolyte phase (V)

Superscript

$\cdot$	volumetric average
a	KOH
b	$K_2Zn(OH)_4$

Subscript

$\pm$	physical property under volumetric average
acc	anode current collector–anode boundary
a	anode, anode–separator boundary, KOH
A	electrochemical reaction
b	$K_2Zn(OH)_4$
B	chemical reaction
c	cathode, cathode–cathode current collector boundary
re	reference condition taken to be the same as the working electrode
ref	reference condition taken as initial condition
s	surface, separator–cathode boundary

References

[1] C.Y. Mak, H.Y. Cheh, G.S. Kelsey, P. Chalilpoyil, J. Electrochem. Soc. 138 (1991) 1607.
[2] J. Euler, W. Nonnenmacher, Electrochim. Acta 2 (1960) 268.
[3] C.Y. Mak, H.Y. Cheh, G.S. Kelsey, P. Chalilpoyil, J. Electrochem. Soc. 138 (1991) 1611.
[4] J.S. Chen, H.Y. Cheh, J. Electrochem. Soc. 140 (1993) 1205.
[5] J.S. Chen, H.Y. Cheh, J. Electrochem. Soc. 140 (1993) 1213.
[6] E.J. Podlaha, H.Y. Cheh, J. Electrochem. Soc. 141 (1994) 15.

[7] E.J. Podlaha, H.Y. Cheh, J. Electrochem. Soc. 141 (1994) 28.
[8] J.S. Newman, Electrochemical Systems, 2nd edn., Prentice Hall, Englewood Cliffs, NJ, 1991.
[9] D. Fan, Ph.D. Dissertation, Texas A&M University, 1991.
[10] D.N. Bennion, AIChE Symp. Ser. 79 (1983) 25.
[11] K.E. Brenan, S.L. Campbell, L.R. Petzold, Numerical Solution of Initial-Value Problems in Differential-Algebraic Equations, North Holland, New York, NY, 1989.
[12] Y. Zhang, H.Y. Cheh, J. Electrochem. Soc. 146 (1999) 850.
[13] Y. Zhang, H.Y. Cheh, J. Electrochem. Soc. 146 (1999) 3566.
[14] G.M. Ostrovsky, Y.M. Volin, E.I. Barit, M.M. Senyavin, Comput. Chem. Eng. 18 (1994) 8.
[15] H. Kahil, F. Dalard, J. Guitton, J.P. Cohen-Addad, Surf. Technol. 16 (1982) 331.
[16] Z. Hong, C. Zhenhai, Xiaxia, J. Electrochem. Soc 136 (1989) 2771.
[17] D.A. Straub, I.E. Grossmann, Comput. Chem. Eng. 14 (1990) 9.
[18] G.J Hahn, S.S. Shapiro, Statistical Models in Engineering, Wiley, 1994.
[19] J.O.'M. Bockris, Z. Nagy, A. Damjanovic, J. Electrochem. Soc. 119 (1972) 285.
[20] R. Pollard, J. Newman, J. Electrochem. Soc. 128 (1981) 491.